Model for the Thermal Performance of Low-Sloped Roofs

K.E. Wilkes, Ph.D., P.E.
*Member **ASHRAE***

ABSTRACT

This paper gives a detailed description of the model named STAR (Simplified Transient Analysis of Roofs) that has been developed at a national laboratory for predicting the heat flows and temperatures within roof systems. STAR is a one-dimensional, finite-difference, transient heat conduction model that can be used on a personal computer. It has full coupling to ambient weather conditions, but can also be used with specified temperature boundary conditions.

The paper also gives results of a validation study in which predictions of the model were compared with temperatures and heat flows that were measured on roof sections at the laboratory's outdoor roof thermal research apparatus. Finally, the paper gives several examples of the application of the model in performing parametric analyses of the thermal performance of roofs. The model is used to predict membrane temperatures and roof heat flows as influenced by variations in parameters such as level of insulation, amount of surface mass, and solar absorptance of the roof surface.

INTRODUCTION

Models play an important role in the operation of the Roof Research Center. They increase the efficiency of costly experimentation by guiding the placement of sensors, identifying critical experiments, and extrapolating the results of experimental data to conditions other than those which were tested. Models are essential to developing an understanding of the complex interactions of the thermal, moisture, and mechanical behaviors of roofs. Finally, models provide tools to aid the design of more energy-efficient and durable roofs.

This paper describes a new model, called STAR (Simplified Transient Analysis of Roofs), which has been developed for predicting heat flows and temperatures within roof systems. The model handles transient one-dimensional heat transfer in multilayer roof systems having temperature-dependent thermal properties, and is fully coupled to ambient weather conditions. It has been implemented on a personal computer and has been designed to be easy to use for a variety of problems. This paper gives details of the mathematical model, a verification of the model by comparing its predictions with existing experimental data, and some examples of its use.

K. E. Wilkes is a member of the Research Staff at the Oak Ridge National Laboratory, Oak Ridge, TN.

MATHEMATICAL MODEL

The mathematical model consists of a standard finite difference analysis of transient one-dimensional heat transfer by conduction through multiple layers of a roof system, with coupling to ambient weather conditions. The finite difference formulation follows that given by Patankar (1980). Each of the layers may have different thermal properties, and the thermal conductivities and specific heats may be taken to be constants or to vary linearly with temperature. The model has provisions for solution of the transient finite difference equations by either classical explicit, fully implicit, or Crank-Nicolson methods. Although all three methods are available, the fully implicit method is recommended to avoid numerical instabilities.

The boundary conditions for the finite difference model may be either specified boundary temperatures or full coupling to the ambient weather or indoor conditions. Specified boundary temperatures are useful for analysis of experimental data, while full coupling to ambient conditions is necessary to analyze hypothetical cases. Coupling to ambient weather conditions is obtained using the following heat balance at the exterior surface of the roof:

$$\alpha Q_{solar} + \epsilon Q_{infrared} + h\,(T_{air} - T_s) - \epsilon\sigma T_s^4 + Q_{latent} + Q_{cond} = 0 \qquad (1)$$

The terms in this equation represent absorbed solar radiation, absorbed incident infrared (sky) radiation, convection from the air to the surface, radiation emitted by the surface, heat delivered to the surface by condensation of moisture (or removed by evaporation), and the heat conducted toward the surface from within the roof system. The quantities α and ϵ are the solar absorptance and infrared emittance of the surface, respectively. The surface is assumed to be gray in the infrared region, so that the infrared absorptance and emittance are equal.

Convection heat transfer from the interior and exterior surfaces is calculated from correlations available in the literature for isolated isothermal flat plates (Holman 1981). These correlations account for the orientation and size of the plate, direction of heat flow (up vs. down), surface-to-air temperature difference, mean (film) temperature, and speed of airflow past the plate. The correlations are given in Table 1 in terms of dimensionless variables. Correlations are used for both natural and forced convection, with a further breakdown for laminar and turbulent flow. The choice between laminar and turbulent correlations is made depending upon the magnitude of the Rayleigh number (for natural convection) or the Reynolds number (for forced convection). Separate coefficients are calculated for natural and forced flow, and a mixed coefficient is calculated by taking the third root of the sum of the cubes of the two separate coefficients (Chen et.al. 1986). Although these correlations rely upon recent research, such as from Holman (1981) and Chen et. al. (1986), there is still considerable uncertainty in the convection coefficients, possibly on the order of 10% to 20%.

The latent heat term accounts for the heat associated with the condensation or evaporation of moisture at the outer surface of the roof. The latent heat term is obtained as the product of the rate of mass transfer at the surface, $\dot{m}_v$, and the latent heat of vaporization of water, h_v. The mass transfer rate is given by

$$\dot{m}_v = h_m\,(W_{air} - W_s) \qquad (2)$$

where W is the humidity ratio of the air or surface and h_m is the mass transfer coefficient. The humidity ratios are calculated from psychrometric relations using known values of the relative humidity and temperature of the air and the temperature of the surface. When condensed moisture is present on the surface, the humidity ratio at the surface is taken to correspond to saturation conditions for the temperature of the surface. The mass transfer coefficient is obtained from the analogy between heat and mass transfer as

$$h_c/(h_m\,C_p) = (\alpha/D)^{2/3} \simeq 1 \qquad (3)$$

where h_c is the convection heat transfer coefficient, C_p is the specific heat of air, α is the thermal diffusivity of air, and D is the coefficient for diffusion of water vapor through air. For this model, h_v has been taken to have a constant value of 1060 Btu/lb.

The model allows incident infrared (sky) radiation to be handled in either of two ways. With the first method, measured values of infrared radiation are used directly in the model, as

is done for the solar radiation. Since measured values are not usually available from weather data, an alternative method based on the work of Martin and Berdahl (1984) is used to calculate an effective sky temperature as a function of the relative humidity, time of day, and cloud cover.

COMPUTER IMPLEMENTATION

The STAR model has been implemented on a personal computer. Details of the numerical algorithms, a flow chart, and a listing of the computer program are given in Wilkes (1989). Two types of input data are needed: basic data to specify the problem and how the model is to be run, and data to specify the boundary conditions. Data for the boundary conditions can be either weather data or measured boundary temperature data.

The basic input data are summarized in Table 2. Two methods of reading these data have been provided. With the first method, the input data are entered interactively on the keyboard, with prompting questions displayed on the monitor. With the other method, the same input data are read from an external file. Both methods are contained in a single computer program. Also, a user interface is being developed to improve the ease of data entry. This will consist of several computer screens on which data are entered by moving the cursor around.

The basic input data include geometric information about the roof: its slope, length, and width. Next are the number of layers in the roof and, for each layer, the name of the material (not used at present), the thickness, number of nodes, thermal conductivity, specific heat, and density. The model is set up to accept the slope and intercept for thermal conductivities and specific heats that vary linearly with temperature.

The program is set up to accept boundary data and calculate results on an hourly basis. However, the time step used in the transient solution can be smaller, with the provision that there be an integer number of time steps per hour. The user may also choose the transient solution method to be used. Finally, the user chooses the type of boundary condition on the outside and inside surfaces, and supplies other information relating to the boundaries, if needed.

Depending upon the type of boundary conditions chosen, either a file containing weather data or a file containing measured temperatures is needed. Weather data used are hourly values of outdoor air temperature, relative humidity, barometric pressure, total solar radiation on horizontal surface, wind speed, and either total incident infrared radiation or cloud amount. Experimental data used are hourly measured values for temperatures at the surfaces and layer interfaces.

The results of the calculations are hourly values of temperatures and heat flows at all interfaces between materials and at the inside and outside surfaces of the roof, and the amount of water accumulated at the outer surface.

COMPARISON OF MODEL WITH EXPERIMENT

The STAR model has been verified by comparing its predictions with experimental data collected at the Roof Thermal Research Apparatus (RTRA), the interior of which is maintained near 75°F. The panel used for comparisons with the model consisted of four 15/16-in sheets of fiberglass insulation over an 18-gauge galvanized steel roof deck. The top surface was sealed with a modified bitumen membrane. The panel was divided into two 4-ft by 4-ft sections. One section was left bare and the other section was covered with concrete pavers. Another bitumen cover was added to the pavers in order to match the radiative properties of the two panel sections. Near the center of each section, thermocouples were located at the exterior boundaries and between each layer of the panel. Calibrated heat flux transducers were located between the two inner layers of insulation near the center of each section. Hourly weather data consisting of the outdoor temperature, relative humidity, wind speed, barometric pressure, incident solar radiation (pyranometer), and incident infrared radiation (pyrgeometer) also were collected at the site.

Two weeks of data were selected for comparison with the model predictions. They correspond to a cool week (January 29-February 4, 1986) and a warm week (May 1-May 7, 1986). During the week in January, the ambient temperature varied between 19° and 69°F and exhibited a warming trend. During May, relatively warm days and cool nights prevailed, with ambient temperatures varying between 35° and 88°F. The January time period exhibited both cloudy and sunny conditions, while the week in May had predominantly clear skies.

The validity of the model was assessed by comparing its predictions with the measured roof heat fluxes. Values used for the geometry and material properties are given in Table 3. The solar absorptance value was determined from in-house measurements, while the other property values were taken from ASHRAE (1985) and NRCA (1988). The thermal conductivity of the insulation was taken to vary linearly with temperature with values of 0.20525 and 0.254 at 0°F and 75°F, respectively. All calculations were performed using the fully implicit technique, using a time step of 0.1 hours. A few runs were made with time steps of one hour and 0.01 hours, with more and fewer nodes to verify that the node spacings and time step used were satisfactory.

As the node spacings or time step is reduced, the numerical accuracy of the calculations should increase, but at the expense of an increase in computational time. An example of the tradeoff between accuracy and computational time is given in Table 4, which contains results for the bare roof for the week in May using weather boundary conditions. This table gives a summation of the positive and negative heat flows over the week, and the run times on a personal computer for various node spacings and time steps. Note that the sign convention used throughout this paper is that heat flows out through the roof are taken as positive. The computer run times are one to two minutes for a time step of one hour, four to eight minutes for a 0.1 hour time step, and one-half to one hour for a 0.01 hour time step. Calculated heat flows are all within about 1% of each other, except for those with a one-hour time step, which are within about 5% of the other values.

In the first step of this assessment, the model was run using measured temperatures for boundary conditions at the inside surface and at various planes within the bare and paver roof panels. Measured and predicted heat flows for the paver roof during the week in winter are shown in Fig. 1, using the temperature measured at the top of the paver as a boundary condition. Note that for all figures, the origin of the time axis is at midnight, and positive heat flows are out through the roof. Overall, the predictions are in very good agreement with the measured heat fluxes, indicating that the heat transfer processes across the stack of insulation, membrane, and paver are being modeled properly. The most noticeable discrepancies are during the cold nighttime hours at the beginning of the week. Based on similar model runs using a constant value of 0.254 for the insulation conductivity, it appears that this remaining discrepancy may be due to uncertainties in the thermal property values at low temperatures. The same level of agreement shown in Figure 1 was also obtained for model runs for the bare roof in winter and for both roofs in May.

As the next step, the weather boundary conditions on the exterior side of the roof were used instead of the measured boundary temperatures. Measured and predicted heat fluxes for the bare roof during the week in winter are shown in Fig. 2. Two predicted curves are given. One used the incident infrared radiation measured on-site in the surface heat balance, while the other used a sky temperature during the nighttime hours that was equal to the outdoor air temperature. The second simulation was done because it was suspected that the nighttime pyrgeometer measurements may have been too low because of condensation of moisture on the instrument. The results in Figure 2 show that the nighttime heat flux is sensitive to the nighttime infrared radiation, but that the two approaches bracket the measured heat fluxes. Other than during the nighttime hours, the predicted and measured values are in very good agreement.

A similar set of runs was performed for the paver roof for the week in January, with the results shown in Figure 3. Again, the predicted heat fluxes are in very good agreement with the measured values, except for the nighttime hours, where the two approaches for the infrared radiation bracket the measured values.

Model predictions for the bare roof in May are compared with measured heat fluxes in Figure 4. For these comparisons, two model runs were made. For Run 1, the measured infrared radiation and a roof solar absorptance of 0.84 were used. For Run 2, the sky radiation model and a lower solar absorptance of 0.7 were used. The figure shows that the two approaches to the infrared radiation bracket the measured nighttime heat fluxes, while the lower solar absorptance produces better predictions during the daytime hours. The same trends were found for the paver roof. Although these observations are not conclusive, they suggest that the

solar absorptance of the outer membrane may have changed between the winter tests and the spring tests as the membrane aged. Alternatively, part of the discrepancies during the daytime hours may be due to uncertainties in the convection coefficients.

EXAMPLES OF USE OF MODEL

Since the model predictions have been shown to be in good agreement with measured values, use of the model to explore other hypothetical cases is justified. In this section, three examples of the use of the model are given. These examples are not meant to be exhaustive, but are given only as an indication of some of the analyses that may be done with the model.

The first example is a simple roof system consisting of a steel deck, a layer of fiberglass insulation, and a membrane. The May weather data used for the model validation were used as boundary conditions, and the model was used to calculate the peak temperature experienced by the outside surface of the membrane and the weekly heat flows out of (positive values) and into (negative values) the roof. Calculated membrane temperatures and heat flows are shown in Figures 5 and 6 for a wide range of insulation levels and membrane solar absorptances. These results show that the solar absorptance has a pronounced effect both on the membrane temperatures and on the heat flows into the building (negative heat flows), but little effect on the heat flows out of the building (positive heat flows) for these weather conditions. On the other hand, the insulation level has a minor effect on the peak membrane temperatures, but a major effect on the heat flows.

The second example is the same as the first, except that surface mass is added on top of the membrane. Figure 7 shows that the addition of surface mass can significantly reduce the peak temperatures experienced by the membrane, while Figure 8 shows that the effect of surface mass on heat flows is significant, but much less than the effect of changing insulation levels.

The third example examines the effect of a woodfiber cover board on reducing the temperature extremes experienced by extruded polystyrene insulation. The base case consisted of 2 in of insulation with a black EPDM membrane, while the other case had a 1/2-in-thick woodfiber board added between the insulation and the membrane. Weather data from Typical Meteorological Year tapes for several locations were used with the model to calculate the hour-by-hour temperature at the top of the insulation for a full year. (Note: the model was transferred to a mainframe computer for these whole-year simulations.) Resulting hourly temperatures were arranged into 5°F bins to produce histograms such as the one shown for Miami in Figures 9 and 10. The effect of the woodfiber board is seen as a reduction in peak temperatures, a reduction in the number of hours at both the extreme hot and extreme cold temperatures, and an increase in the number of hours at mild temperatures. Histograms for other climates show the large qualitative differences in numbers of hours at various temperatures, but show that peak temperatures are similar for different climates.

SUMMARY AND CONCLUSIONS

An easy-to-use and computationally efficient computer model for the thermal performance of roofs has been developed and implemented on a personal computer. The model has been verified by comparing its predictions against experimental data taken at the RTRA during a cool week in January and February and during a warm week in May. The data were obtained on a roof section insulated with fiberglass insulation and covered with a modified bitumen membrane and on a similar roof section with a layer of concrete pavers added on top. From comparisons of predicted and measured membrane temperatures and heat flows, it is concluded that the models capture the most important features of the diurnal cycles, the trends in weather during the weekly periods, and major differences between the weather conditions in the two weeks. It also appears that significant improvements can be obtained with refinements in the values for incident infrared radiation and possibly for the solar absorptance after aging. The usefulness of the model in performing parametric analyses for various roof systems has been demonstrated by several examples. The examples have demonstrated the relative importance of membrane solar absorptance, insulation level, and surface mass in determining peak membrane temperatures and heat flows through the roof. Another example demonstrated the reduction in peak insulation temperature obtained by adding a woodfiber coverboard.

While the STAR model is useful at present, it will continue to be developed. Work is under way to make the model more user friendly. In addition, the model will be extended to include migration of moisture and will be coupled with other models for determining induced mechanical strains and stresses in the roof system.

ACKNOWLEDGEMENTS

This work was supported by the Office of Buildings and Community Systems, U.S. Department of Energy, under Contract No. DE-AC05-840R21400 with Martin Marietta Energy Systems, Inc.

REFERENCES

ASHRAE. 1985. ASHRAE handbook--1985 fundamentals, Atlanta: American Society of Heating, Refrigerating, and Air-Conditioning Engineers, Inc.

Chen, T.S.; Armaly, B.F.; and Ramachandran, N. 1986. "Correlations for laminar mixed convection flows on vertical, inclined, and horizontal flat plates." ASME Journal of Heat Transfer, Vol. 108, pp. 835-840.

Holman, J.P. 1981. Heat transfer, 5th ed., pp. 191, 202, 272-286. New York: McGraw-Hill.

Martin, M., and Berdahl, P. 1984. "Characteristics of infrared sky raiation in the United States." Solar Energy, Vol. 33, pp. 321-336.

NRCA. 1988. NRCA roofing materials guide, Vol. 13. Rosemont, IL: National Roofing Contractors Association.

Patankar, S.V. 1980. Numerical heat transfer and fluid flow. New York: Hemisphere.

Wilkes, K.E. 1989. Model for roof thermal performance, ORNL/CON-274. Oak Ridge, TN: Oak Ridge National Laboratory.

TABLE 1

Correlations for Convection Coefficients (Holman 1981)

I. Natural Convection:

A. Horizontal surface, heat flow up

$Nu = 0.54\ Ra^{1/4}$ for $Ra < 8 \times 10^6$

$Nu = 0.15\ Ra^{1/3}$ for $Ra > 8 \times 10^6$

B. Horizontal surface, heat flow down

$Nu = 0.58\ Ra^{0.2}$

C. Vertical surface

$Nu = 0.59\ Ra^{1/4}$ for $Ra < 1 \times 10^9$

$Nu = 0.10\ Ra^{1/3}$ for $Ra > 1 \times 10^9$

D. Nearly horizontal surface (tilt angle less than 2 degrees), heat flow down

$Nu = 0.58\ Ra^{0.2}$

E. Tilted surfaces (greater than 2 degrees tilt), heat flow down

$Nu = 0.56\ (Ra \cos(\varphi))^{1/4}$ φ = tilt angle

F. Tilted surface, heat flow up

$Nu = 0.56\ (Ra \cos(\varphi))^{1/4}$ for $Ra/Pr < Gr_c$

$Nu = 0.14\ (Ra^{1/3} - (Gr_c\ Pr)^{1/3}) + 0.56\ (Ra \cos(\varphi))^{1/4}$ for $Ra/Pr > Gr_c$

$Gr_c = 1 \times 10^6$ for $\varphi < 15$ degrees

$Gr_c = 10^{**}(\varphi/(1.1870 + 0.0870*\varphi))$ for 15 degrees $< \varphi < 75$ degrees

$Gr_c = 5 \times 10^9$ for $\varphi > 75$ degrees

II. Forced Convection

$Nu = 0.664\ Pr^{1/3}\ Re^{1/2}$ for $Re < 5 \times 10^5$

$Nu = Pr^{1/3}\ (0.037\ Re^{0.8} - 850)$ for $Re > 5 \times 10^5$

TABLE 2

Data Entered by Keyboard or from External File

1. Slope of roof, inches of rise per foot of run.
2. Length and width of roof, feet.
3. Number of layers in roof, limit of 20.
4. For each layer of the roof,
   a. Name of material
   b. Thickness, inches.
   c. Number of nodes, limit of 100.
   d. Thermal conductivity, slope and intercept for a linear variation with temperature, Btu-in./(hr-ft^2-^{o}F).
   e. Specific heat, slope and intercept for a linear variation with temperature, Btu/(lb-^{o}F).
   f. Density, lb/ft^3.
5. Size of time step, expressed as an integer number of time steps per hour of simulated time.
6. Choice of transient solution method: enter 0 for explicit, 0.5 for Crank-Nicolson, or 1.0 for fully implicit.
7. Choice of boundary conditions on outside surface: enter 0 for specified temperature or 1 for weather boundary conditions.
8. Solar absorptance and infrared emittance (only if weather boundary conditions are chosen), dimensionless.
9. Choice of a outside convection coefficient: enter 0 for user specified outside convection coefficient, or 1 for coefficients obtained from the built-in correlations (only if weather boundary conditions are chosen).
10. User specified outside convection coefficient (if needed), Btu/(hr-ft^2-^{o}F).
11. Choice to include or ignore the effects of latent heats at the outside surface: enter 0 to ignore or 1 to include.
12. Choice of boundary condition on inside surface: enter 0 for specified temperature or 1 for room conditions.
13. Indoor temperature (if room conditions chosen), ^{o}F.
14. Choice of inside convection coefficient: enter 0 for user specified inside convection coefficient, or 1 for coefficient obtained from correlations (only if room conditions are chosen).
15. User specified inside convection coefficient (if needed), Btu/(hr-ft^2-^{o}F).

TABLE 3

Material Properties and Geometric Values Used in Models

Material	Thickness in.	Number of Nodes	Thermal Conductivity, BTU-in/(hr-ft^2-^{o}F)	Specific Heat, BTU/(lb-^{o}F)	Density, lb/ft^3
Modified Bitumen*	0.160	1	1.14	0.35	67.5
Concrete	1.875	4	12.0	0.22	140.0
Modified Bitumen*	0.2225	1	1.14	0.35	67.5
Fiberglass Insulation	3.75	8	0.254	0.23	13.2

* Solar Absorptance = 0.84
Infrared Emittance = 0.9

TABLE 4

Sensitivity of Heat Flow Calculations to Node Spacing and Time Step (For bare roof in May using weather boundary conditions)

Number of Nodes	Time Step, hours	Weekly Heat Flows, Btu/ft^2 Positive	Negative	Run Time, minutes
5	0.01	193.90	268.39	28.2
5	0.1	192.94	267.49	4.5
5	1	185.38	259.80	1.2
9	0.01	194.76	270.14	35.8
9	0.1	193.81	269.24	5.3
9	1	186.47	261.83	1.4
18	0.01	195.01	270.58	52.2
18	0.1	194.06	269.68	7.5
18	1	186.77	262.35	1.8

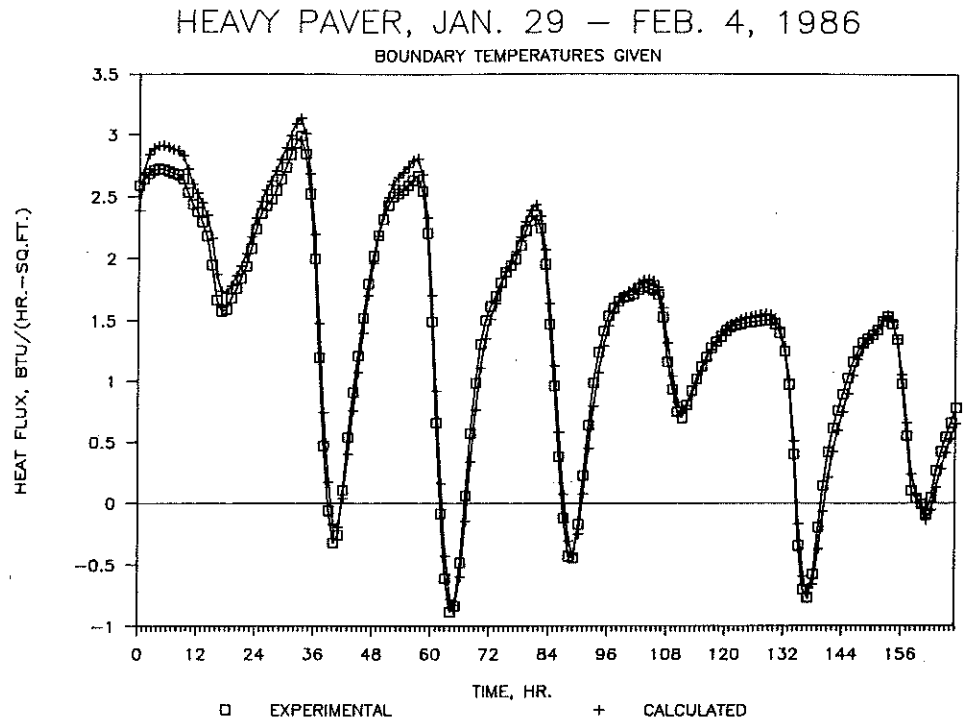

Figure 1. *Comparison of predicted and measured roof heat fluxes for paver roof in cool weather with given boundary temperatures at top of paver (For all figures, positive heat flows are out of the roof. The origin of the time axis is at mid- night.)*

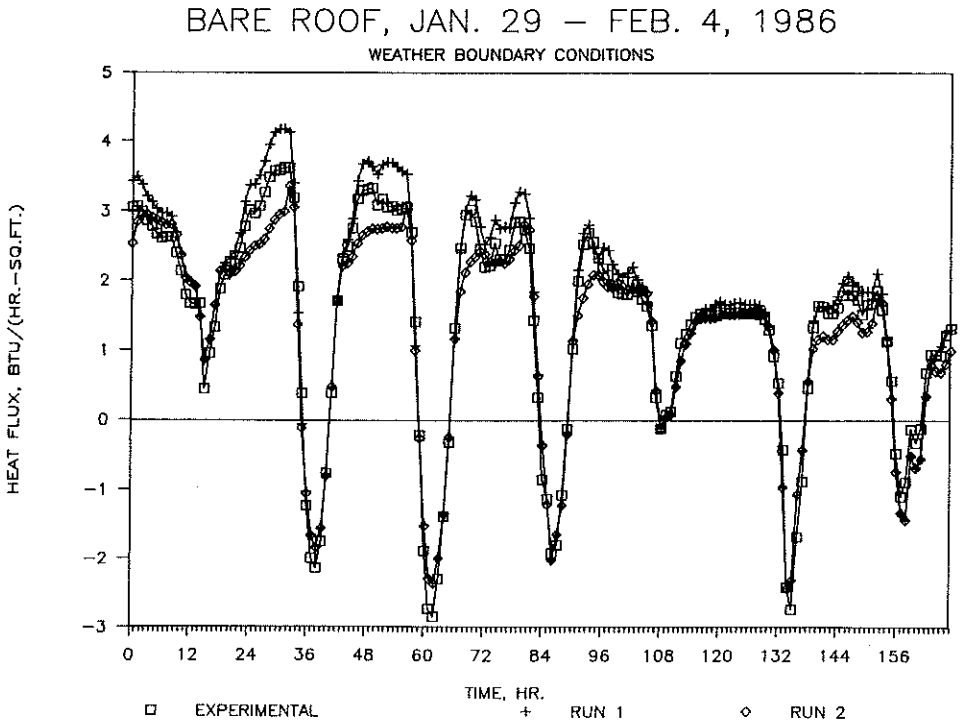

Figure 2. *Comparison of predicted and measured roof heat fluxes for bare roof in cool weather with weather boundary conditions. Run 1 uses on-site measured infrared radiation; Run 2 uses nighttime sky temperature equal to air temperature.*

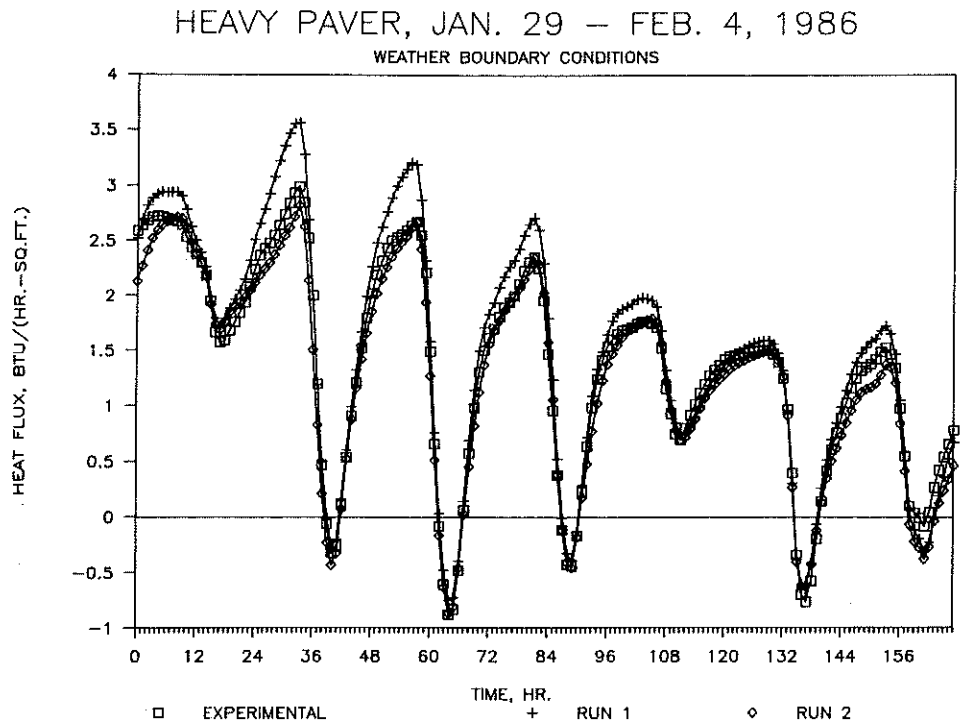

Figure 3. *Comparison of predicted and measured roof heat fluxes for paver roof in cool weather with weather boundary conditions. Run 1 uses on-site measured infrared radiation; Run 2 uses nighttime sky temperature equal to air temperature.*

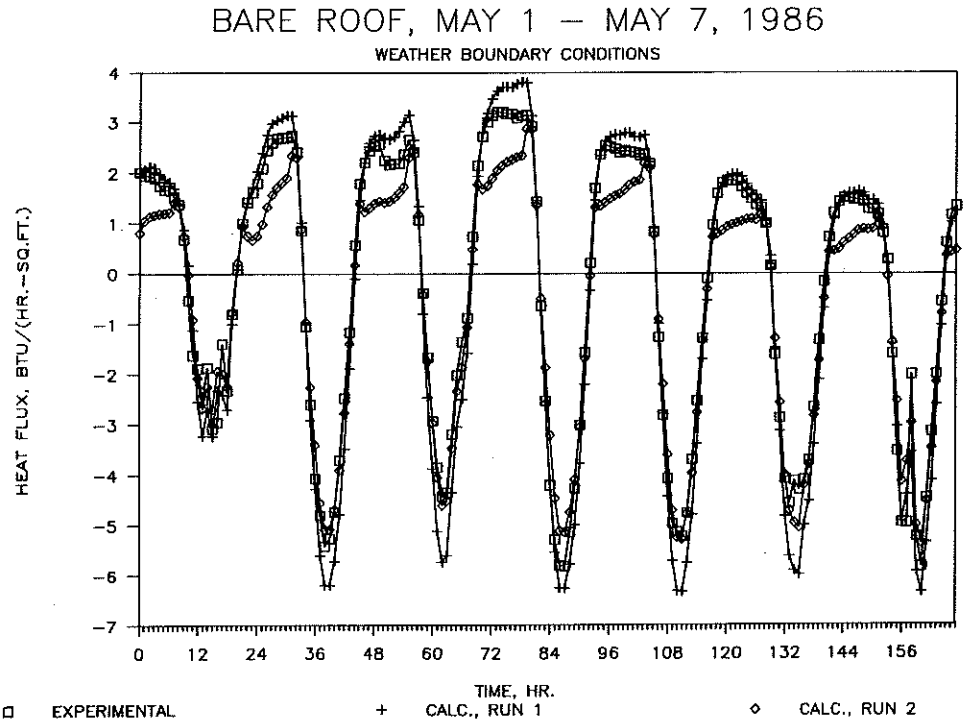

Figure 4. *Comparison of predicted and measured roof heat fluxes for bare roof in warm weather with weather boundary conditions. Run 1 uses on-site measured infrared radiation and solar absorptance of 0.84; Run 2 uses nighttime sky temperature equal to air temperature and solar absorptance of 0.7.*

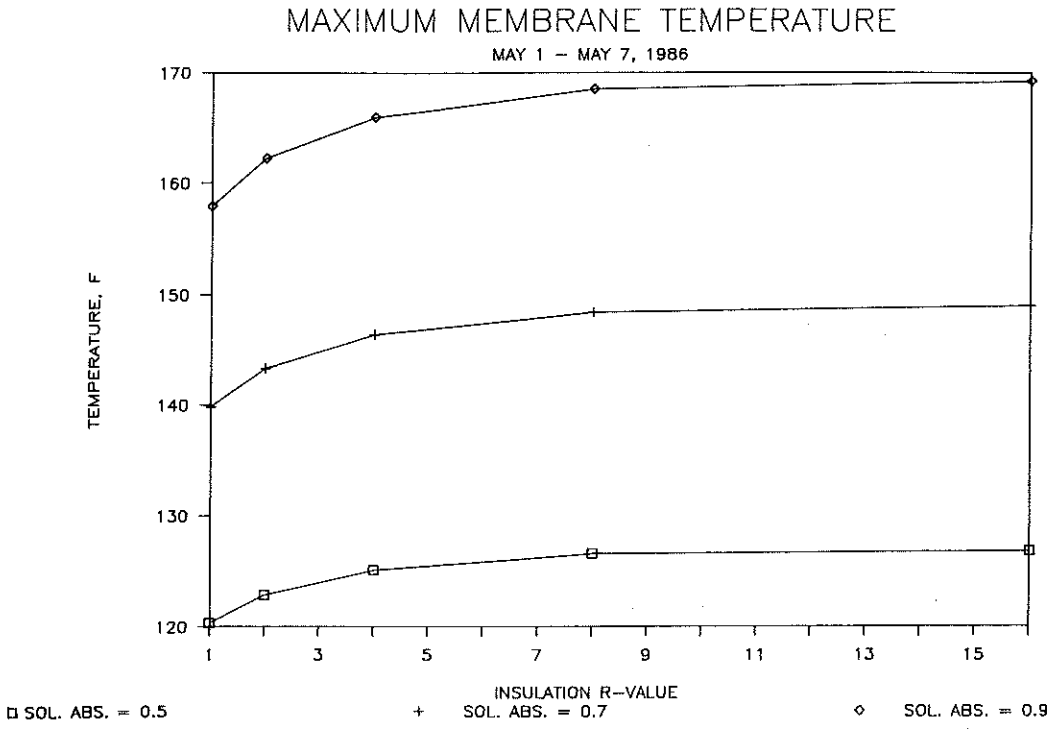

Figure 5. *Predicted effect of solar absorptance and insulation level on peak membrane temperature using weather data from May 1-7, 1986*

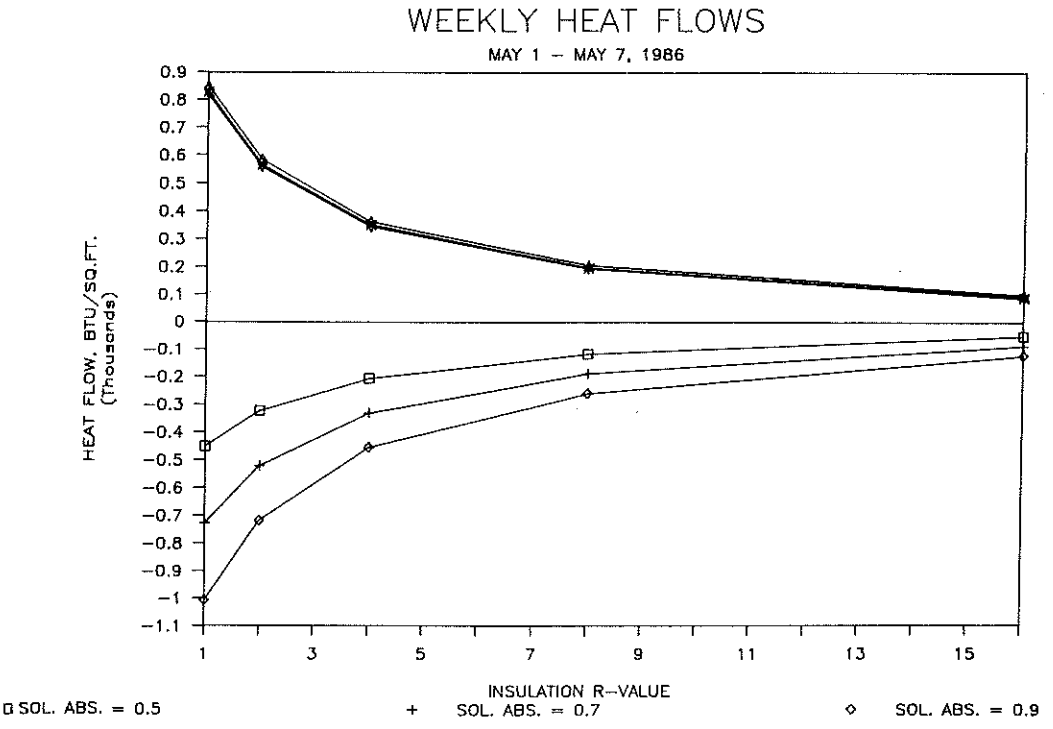

Figure 6. *Predicted effect of solar absorptance and insulation level on heat flows out of (positive) and into (negative) a roof using weather data from May 1-7, 1986*

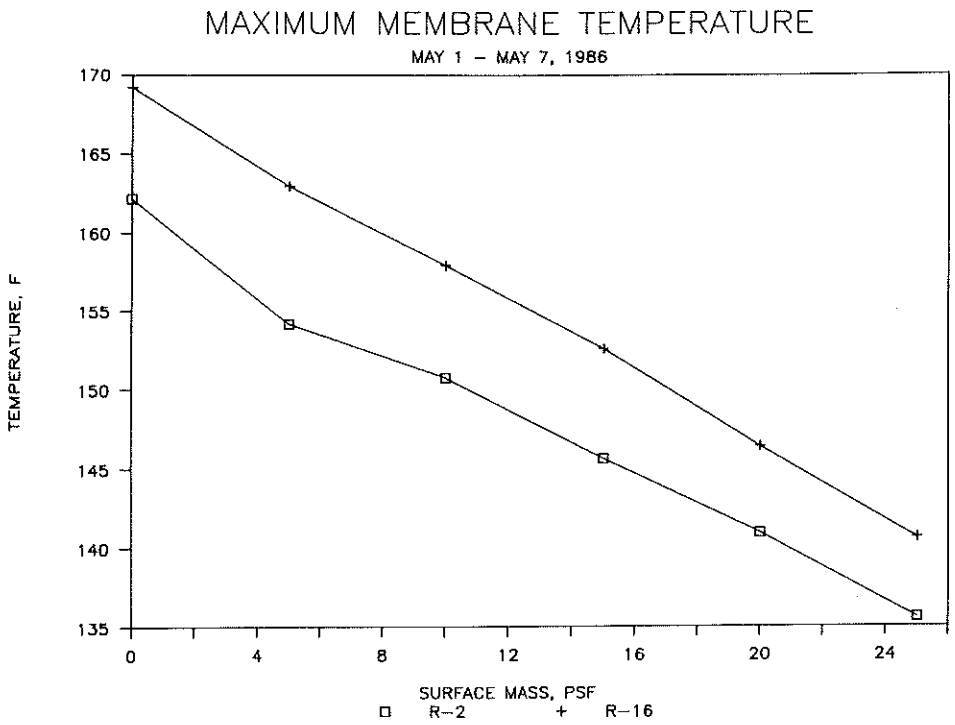

Figure 7. *Predicted effect of surface mass and insulation level on peak membrane temperature using weather data from May 1-7, 1986*

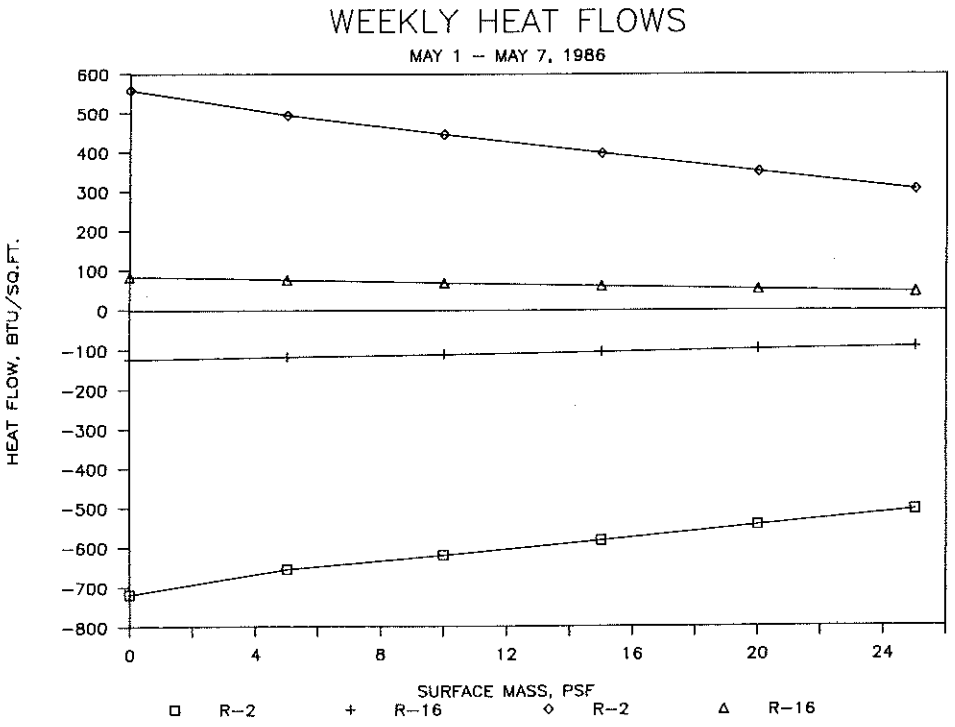

Figure 8. *Predicted effect of surface mass and insulation level on heat flows out of (positive) and into (negative) a roof using weather data from May 1-7, 1986*

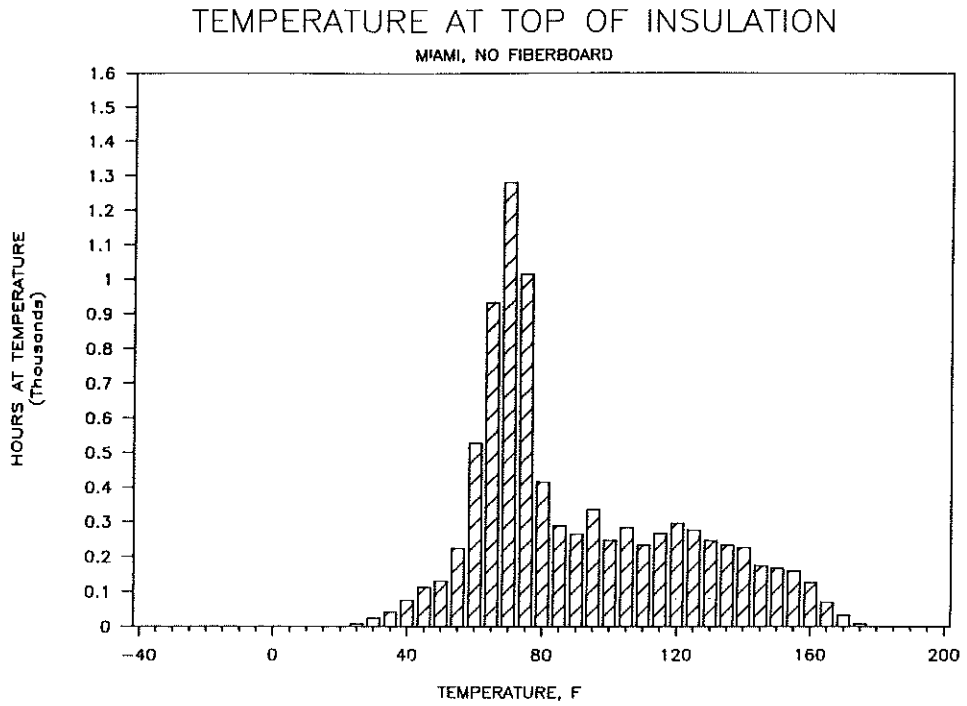

Figure 9. *Frequency of hourly insulation temperatures for roof without woodfiber coverboard using TMY weather data for Miami, FL*

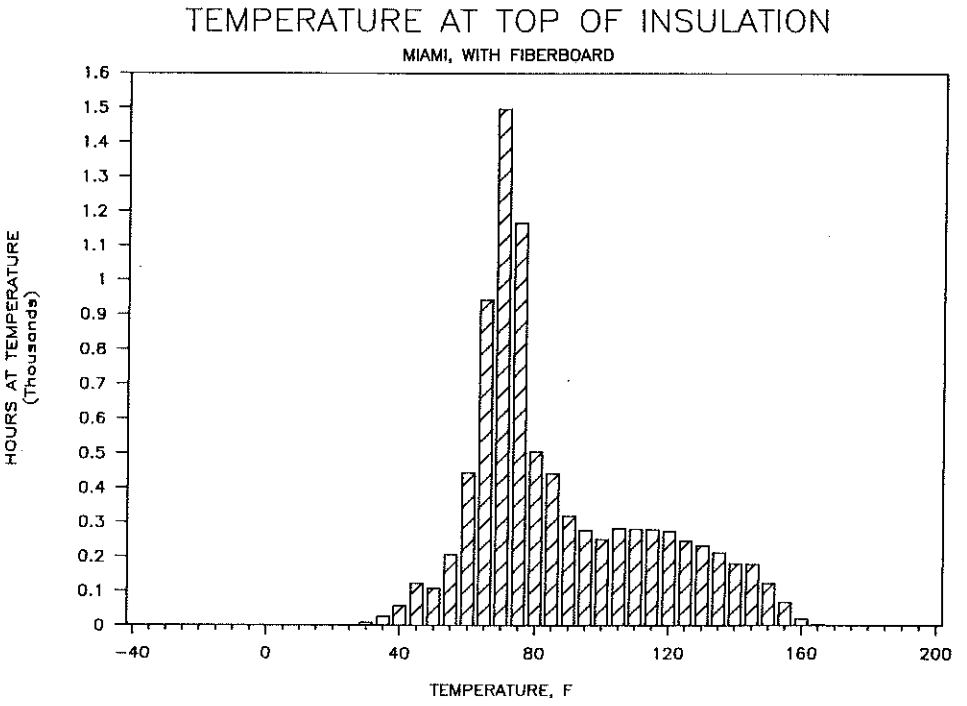

Figure 10. *Frequency of hourly insulation temperatures for roof with woodfiber coverboard using TMY weather data for Miami, FL*